Spatial and seasonal variation in wave attenuation over *Zostera noltii*

M. Paul[1] and C. L. Amos[1]

Received 11 November 2010; revised 5 May 2011; accepted 17 May 2011; published 23 August 2011.

[1] Wave attenuation is a recognized function of sea grass ecosystems which is believed to depend on plant characteristics. This paper presents field data on wave attenuance collected over a 13 month period in a *Zostera noltii* meadow. The meadow showed a strong seasonality with high shoot densities in summer (approximately 4,600 shoots/m^2) and low densities in winter (approximately 600 shoots/m^2). Wave heights and flow velocities were measured along a transect at regular intervals during which the site was exposed to wind waves and boat wakes that differ in wave period and steepness. This difference was used to investigate whether wave attenuation by sea grass changes with hydrodynamic conditions. A seasonal change in wave attenuation was observed from the data. Results suggest that a minimum shoot density is necessary to initiate wave attenuation by sea grass. Additionally, a dependence of wave attenuation on hydrodynamics was found. Results suggest that the threshold shoot density varies with wave period and a change in energy dissipation toward the shore was observed once this threshold was exceeded. An attempt was made to quantify the bed roughness of the meadow; the applicability of this roughness value in swaying vegetation is discussed. Finally, the drag coefficient for the meadow was computed: A relationship between wave attenuance and vegetation Reynolds number was found which allows comparing the wave attenuating effect of *Zostera noltii* to other plant species.

Citation: Paul, M., and C. L. Amos (2011), Spatial and seasonal variation in wave attenuation over *Zostera noltii*, *J. Geophys. Res.*, *116*, C08019, doi:10.1029/2010JC006797.

1. Introduction

[2] Wave attenuation has been recognized as an important ecosystem function of sea grass meadows [*Madsen et al.*, 2001] that contributes to the economic value of such ecosystems [*Koch et al.*, 2009]. Attempts have been made to quantify the economic value of ecosystems and at present, the valuation process is based on the assumption that ecosystem functions vary linearly with plant characteristics [*Barbier et al.*, 2008]. However, laboratory experiments showed that plant traits such as shoot density and canopy height lead to a nonlinear response in wave height reduction [*Bouma et al.*, 2010; *Fonseca and Cahalan*, 1992] and linearity may therefore be an inappropriate approximation [*Koch et al.*, 2009].

[3] While nonlinear relationships have been observed in laboratory studies [*Méndez et al.*, 1999; *Bouma et al.*, 2010], only few field studies are available to quantify the nonlinear response of wave attenuation to changing vegetation characteristics. To date, most studies were carried out on short time scales and during summer months, when above ground biomass was high. Such results cannot be applied to the whole year if a species shows a high seasonality [*Widdows et al.*, 2008]. For example, *Verduin et al.* [2002] sampled for five to ten minutes in an *Amphibolis antarctica* meadow and repeated data collection in spring and autumn; *Bradley and Houser* [2009] studied a *Thalassia testudinum* bed and collected data for a duration of seven hours in early autumn while *Prager and Halley* [1999] acquired data for two days in late autumn in a *Thalassia* meadow. For the sea grass *Ruppia maritima* ten day deployments were carried out in August [*Ward et al.*, 1984], and June and October [*Newell and Koch*, 2004]. While the combined interpretation of those studies would provide a better understanding of the affect of changes in *Ruppia maritima* on wave attenuation, none of them includes the winter state with low above ground biomass.

[4] In addition to the temporal scale, the spatial distribution needs to be considered when assessing the nonlinear relationship between wave attenuation and vegetation. Previous studies on submerged vegetation found an exponential wave decay with distance into the vegetation [*Kobayashi et al.*, 1993; *Bouma et al.*, 2010; *Möller et al.*, 1999] and that this exponential relationship changed with canopy height and density [*Bouma et al.*, 2010; *Newell and Koch*, 2004]. While individual field studies have addressed the change of wave decay with distance from the meadow edge on short timescales [*Bradley and Houser*, 2009], no data are yet available to confirm its dependence on sea grass characteristics under field conditions.

[5] In the field, sea grass meadows are exposed to a wide range of wave conditions. Depending on the site, they

[1]National Oceanography Centre, University of Southampton, Southampton, UK.

0148-0227/11/2010JC006797

experience long period ocean swell, locally generated short period wind waves or boat wakes. Boat wakes can lead to erosion along otherwise stable coastlines, because they have a higher height/length ratio than natural waves [*Fonseca and Cahalan*, 1992] which may also lead to a different interaction with sea grass. An understanding of this interaction would be desirable for planning new boat activity in coastal regions as it would allow estimations of wake impact on the coast [*Fonseca and Cahalan*, 1992]. However, boat wake attenuation over sea grass has not been investigated in detail [*Ciavola*, 2005].

[6] Several formulas exist to describe wave attenuation and the associated energy dissipation caused by bed features [e.g., *Nielsen*, 1992; *Madsen*, 1994]. These formulas were initially developed for monochromatic wave conditions [*Jonsson*, 1966]; *Madsen* [1994] extended them to spectral waves to make them applicable to more natural conditions. All models use a hydraulic length scale k_N to describe bed roughness. For flat beds, k_N equals the Nikuradse sand grain roughness, and an equivalent bed roughness is used when bed forms are present [*Kamphuis*, 1975]. This approach is valid for a wide variety of bed features; *Mathisen and Madsen* [1996a, 1996b, 1999] applied it to evenly spaced triangular bars in a wave flume and it has been successfully used to estimate the bed roughness of a coral reef flat [*Lowe et al.*, 2005]. However, the models are based on the assumption that k_N is constant and independent of hydrodynamic conditions. Depending on the species, sea grass can be flexible and it is known to sway in an oscillating fashion under waves, changing its shape throughout a wave cycle. It is not yet known how this movement affects the plant's roughness [*Bradley and Houser*, 2009; *Manca*, 2010] and it is therefore uncertain, whether a constant k_N can be applied to vegetated areas.

[7] An alternative method to describe wave energy dissipation caused by vegetation is based on the drag individual plants pose on the flow [*Dalrymple et al.*, 1984]. The model estimates the drag per unit plant area which makes it independent of plant parameters such as height and density. It would therefore allow comparison of the wave attenuating effect of different plant species. A weakness of the model is, however, that is assumes the vegetation to be rigid. *Méndez et al.* [1999] examined the effect plant motion has on vegetation drag. They applied their theory to data from a laboratory study on artificial kelp [*Asano et al.*, 1988] and found that a model which assumes vegetation rigidity underestimates the drag coefficient. The same was found when the model was applied to field data from a *Thalassia testudinum* bed [*Bradley and Houser*, 2009]. However, *Bradley and Houser* [2009] also showed that the simplified model by *Dalrymple et al.* [1984] is a reasonable first approximation.

[8] The studies described above indicate that there is a systematic relationship between sea grass attributes and wave attenuation across species. However, the magnitude of parameters differs between species, as a difference in plant morphology will affect the plant's wave attenuating capacity. The same was found for the effect of vegetation on unidirectional flow where quantitative results cannot be transferred from one species to another [*Fonseca and Fisher*, 1986]. Consequently, wave attenuating parameters need to be quantified for each sea grass species separately.

[9] This paper describes the results of a series of field experiments carried out across a *Zostera noltii* meadow over a period of 13 months in order to assess the change in wave attenuation throughout a year. From this data, bed roughness and vegetation drag were estimated and the applicability of the relevant formulas was evaluated.

2. Study Site

[10] The measurements were carried out within a *Zostera noltii* meadow on Ryde Sand, an intertidal extension of a recreational beach on the north coast of the Isle of Wight, UK (Figure 1). *Zostera noltii* is a temperate, intertidal sea grass species with a preferred growth depth between high and low water neaps, however, it can be found in depths to 5 m in the Mediterranean [*Curiel et al.*, 1996; *Van Lent et al.*, 1991; *Auby and Laborg*, 1996]. Its ribbon-shaped leaves are 0.5–1.5 mm wide and 6–22 cm long [*Phillips and Meñez*, 1988] and above ground biomass shows a strong seasonality of high values in summer and low values in winter [*Curiel et al.*, 1996]. Shoots grow from a rhizome system which builds a dense mesh by branching in almost every node [*Brun et al.*, 2006]. The root/rhizome system is located approximately 3–5 cm below the sediment surface [*Duarte et al.*, 1998] and its biomass remains constant throughout the year [*Pergent-Martini et al.*, 2005].

[11] Ryde Sand has a triangular shape, it is approximately 2.5 km long and the central part reaches approximately 2 km into the Solent. It is composed of fine sand [*Tonks*, 2008] and slopes gently (1:550) toward the adjacent navigation channel. The western half of the sand flat is covered by approximately 40 ha of reticulate to continuous *Zostera noltii* meadow which extends from +2.5 to 0 m Chart Datum (CD). At the lower boundary a succession by *Zostera marina* can be observed, but its extent is unknown. The *Zostera noltii* meadow is dissected by a hovercraft route and a pier that serves as ferry terminal. The pier is built on stilts that have a diameter of 25 cm. The stilts are arranged in rows of six parallel to the shore and the spacing between rows is 5.5 m. Refraction and reflection from these structures could not be observed *in situ* and their effects were not evident in bed forms during low tide. Hence, the pier is considered to have only a minor effect on local waves. This study was carried out west of the pier where little recreational use in the form of small vessels takes place.

[12] The sand flat is sheltered from swell from the English Channel by the Isle of Wight and the study site is exposed to two main sources of waves: (1) wind waves generated by prevailing NW winds with 2–4 s periods and (2) boat waves caused by the ferries arriving and departing from the pier head with 10 s periods. The tidal range is 4 m during spring tides and 2 m during neap tides with the tidal flow peaking at high and low water indicating a progressive wave.

3. Materials and Methods

3.1. Data Collection

[13] The site was visited monthly during spring low tide over a 13 month period from October 2008 to October 2009. During each visit shoot density was measured at four stations randomly chosen within a defined 50 × 50 m region using a 0.3 × 0.3 m quadrate. Additionally, the length of 10

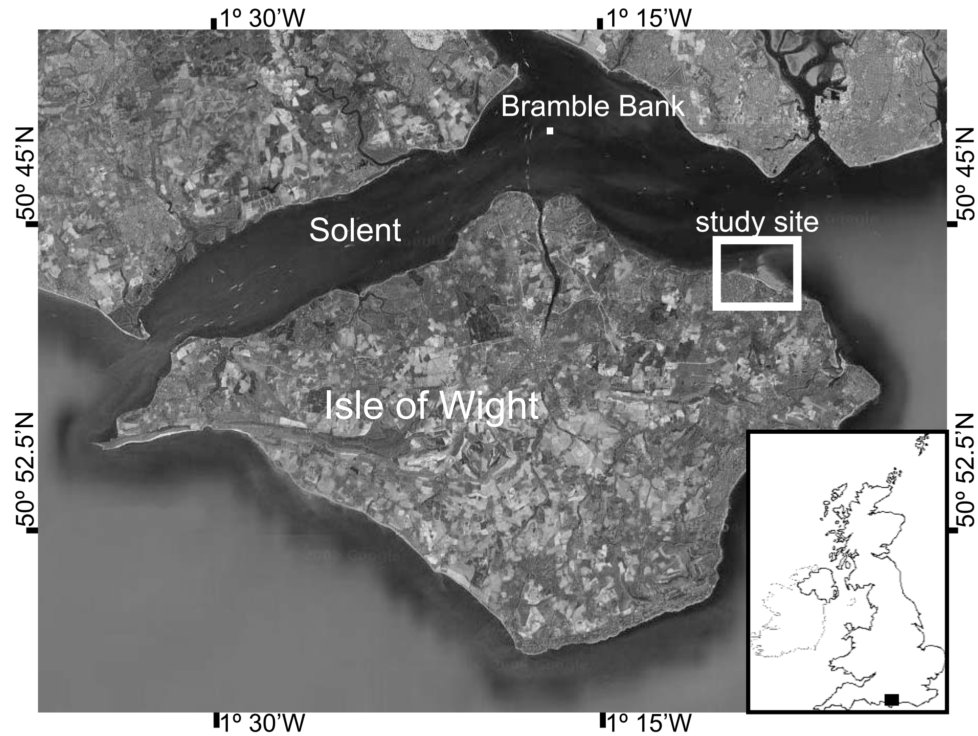

Figure 1. Ryde Sand on the north coast of the Isle of Wight. The box highlights the whole sand flat.

randomly chosen leaves was measured at each station to obtain a record of leaf length variation over the growth cycle. During the October 2008 visit, only one station was sampled due to adverse weather conditions. Five times during the data collection period wave and flow data were collected over two consecutive tidal cycles with deployment and recovery taking place during low tide (Table 1). During each deployment instruments were arranged along a cross-shore transect (Figure 2) approximately 30 m west of the pier. This proximity to the pier was chosen for two practical reasons: (1) It protected the instruments from possible recreational traffic and (2) it extended the transect as far as possible as some instruments had to be connected to the logging station on the pier through 130 m cables. The transect was aligned with the incoming boat wakes at 170° to capture these waves as accurately as possible. This set the transect oblique to prevailing winds, but the majority of wind waves were still captured along the transect and within a wave angle of ±20° of it due to natural variation in the wind field. Stations were between 30 and 95 m apart and an optical

Table 1. Observed Significant Wave Height H, Period T, and Wavelength L for All Deployments

Dates of Deployment	Mean H_s [m]	Max H_s [m]	Mean T [s]	Mean L [m]
25–26 February 2009	0.05	0.15	4.96	19.19
26–27 May 2009	0.07	0.16	3.23	11.55
7–8 July 2009	0.07	0.18	3.11	10.82
7–8 October 2009	0.06	0.13	3.96	15.24

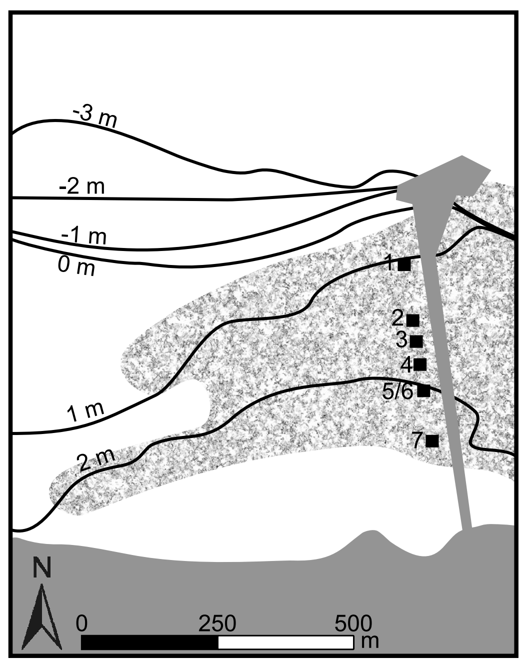

Figure 2. Instrument locations and sand flat bathymetry. Bathymetry is relative to Chart Datum, 0 m marking the boundary between the intertidal and subtidal zones. The shaded area indicates known distribution of sea grass. Note that stations 5 and 6 are at the same location but refer to different types of instruments.

level was used to record their elevations with respect to Chart Datum.

[14] For all but the May deployment three Electromagnetic Current Meters with an integrated Seapoint Sensor (EMCM, Valeport Model 808) were used to sample sea surface elevation and two dimensional horizontal flow velocities at stations 1, 3 and 5. They were mounted on quadropods with the pressure sensor positioned 0.35 m and the current meter 0.13 m above the seabed. They were set to sample at 4 Hz in bursts of 8.5 minutes every 13 minutes. From February 2009 onwards, four pressure transducers (PDCR 1830, Druck Ltd.) were added to the transect at stations 2, 4, 6 and 7. Their sensors were placed directly on the seabed and were connected to a power supply and logging station on the adjacent pier through cables. They sampled continuously at 8 Hz, however, data acquisition was restricted to water depths <2.7 m due to the operating range of the PDCRs. In May, 3D velocity data were obtained using an Acoustic Doppler Velocimeter (ADV, Nortek Vectrino) at station 6, sampling continuously at 25 Hz. Barometric data were obtained from an offshore station on Bramble Bank (www.bramblemet.co.uk), 12 km northwest of Ryde (Figure 1).

3.2. Data Analysis

3.2.1. Wave Conditions

[15] Data from all instruments were split into synchronous five minute intervals with a minimum of 1200 samples per interval. Velocities from the EMCMs were converted into North and East components using the instrument internal compasses. Pressure data from all stations were used to estimate the wave energy spectrum applying Welch's periodogram method. Each interval was split into four segments with 50% overlap and a Hanning window was applied to each segment to reduce spectral leakage. Linear wave theory was applied, although nonlinearities may be present due to shallow water depths and effects of the vegetation field. However, recent studies under similar conditions showed that it is a valid first approximation for wind waves [*Bradley and Houser*, 2009; *Lowe et al.*, 2007; *Mullarney and Henderson*, 2010] as well as boat wakes [*Koch*, 2002; *Garel et al.*, 2008; *Ciavola*, 2005]. The segments were then averaged to obtain a smoothed pressure spectrum S_{pr} with a bandwidth of Δf_b = 1/128 Hz which was converted to an energy density spectrum S_f:

$$S_{f,j} = \left[\frac{\cosh k_j h}{\rho g \cosh k_j (h - z)}\right]^2 S_{pr,j} \tag{1}$$

where the index j denotes the frequency component, h is mean water depth, z is the vertical distance of the pressure sensor above the seabed, ρ is water density, g is gravity and k is wave number according to the dispersion relation

$$\omega^2 = gk \tanh kh \qquad \text{where} \qquad \omega = \frac{2\pi}{T} \tag{2}$$

where T is the wave period.

[16] Velocity and pressure spectra at stations 1, 3 and 5 were used to obtain wave direction and directional spread. Following the method of *Gordon and Lohrmann* [2001], a 4-quadrant arc tangent was applied to the real parts of the pressure-velocity cross-spectra for the east (CS_{pu}) and north (CS_{pv}) velocity components to obtain wave direction D = arctan2(CS_{pu}, CS_{pv}). Wave spreading (spr) was computed according to

$$spr = \sqrt{\frac{1 - R}{2}} \qquad \text{where} \qquad R = \sqrt{\frac{(CS_{uu} - CS_{vv})^2 + 4CS_{uv}^2}{(CS_{uu} + CS_{vv})^2}} \tag{3}$$

where CS_{uu} and CS_{vv} are velocity component power spectra and CS_{uv} is the cross spectrum of the u and v velocity components [*Krogstad et al.*, 1998]. For the May deployment, the same method was applied using the ADV's velocity data together with the pressure data from station 6.

[17] The total energy in the wave spectrum was determined to obtain the zero order moment and hence significant wave height H_s for each five minute interval:

$$H_s = 4\sqrt{\sum_{j=1}^{M} S_{f,j} \Delta f_b} \tag{4}$$

where M is the total number of frequency components.

[18] All instruments were deployed along the same transect. For processing, however, they were split into two groups according to instrument type to avoid inaccuracies caused by differences in instrument operation. The respective groups consist of stations 2, 4, 6 and 7 for the PDCRs and stations 1, 3 and 5 for the EMCMs. Results from both groups were subsequently combined for analysis unless stated otherwise.

3.2.2. Wave Dissipation

[19] Waves interact with the seabed when traveling toward the shore. The main impacts on waves that can cause a change in shape or contained energy are breaking, reflection, shoaling and bottom friction [*Madsen*, 1976]. The sand flat was sloping very gently (~1:550) and hence slope related impacts such as breaking, reflection and shoaling are expected to have a low impact on approaching waves. Breaking of random waves is controlled by water depth; previous studies have shown that linearity is a valid approximation [*Thornton and Guza*, 1982; *Soulsby*, 1997]:

$$H_{rms} = \gamma h \tag{5}$$

where H_{rms} is the root-mean-square wave height and γ is a critical breaking parameter. Recent studies have found γ = 0.2–0.6 for planar and gentle sloping (<1:100) beaches [*Raubenheimer et al.*, 2001, 1996; *Lentz and Raubenheimer*, 1999]. Breaking was observed visually during deployments only when h was too low for the instruments to record accurately. To exclude any effect through partial breaking at higher water depths, data with γ > 0.2 were removed from the present data set.

[20] Reflection occurs over sloping bathymetries; the steeper the slope, the more wave energy will be reflected [*Battjes*, 1974; *Magne et al.*, 2005]. Reflection in this study could be neglected, because the sand flat slope was ~1:550 and comparison with results for linear ramps showed that reflection at such shallow slopes are negligible [*Magne et al.*, 2005]. Possible reflection from the meadow itself was minimized by positioning all stations of the instrumented transect within the meadow and thus excluding the meadow

edge which has a high potential to cause reflection [*Bradley and Houser*, 2009]. Moreover, it has been shown that within a meadow, wave energy reflection by vegetation is negligibly small [*Méndez and Losada*, 2004; *Méndez et al.*, 1999]. Shoaling, on the other hand, was taken into account and its impact was removed from each frequency component of the wave spectrum at stations 2–7 based on the spectrum of the previous station [*Dean and Dalrymple*, 1991]:

$$H_n = H_{n-1} K_s \qquad \text{where} \qquad K_s = \sqrt{\frac{C_{g,n-1}}{C_{g,n}}} \tag{6}$$

where K_s is the shoaling coefficient and n indicates the number of the shore ward station. Once breaking, reflection and shoaling have been considered, a change in wave height between stations along the instrumented transect could be used to estimate bottom friction following the approach of *Lowe et al.* [2005]. Bottom friction will act on waves in shallow water and will reduce the wave energy flux toward the shore. Wave energy flux is defined as:

$$F = EC_g \tag{7}$$

where E is the wave energy density and C_g is the group velocity and can be obtained for each frequency component j following linear wave theory:

$$E_j = \frac{1}{2}\rho g a_j^2 \tag{8}$$

$$C_{g,j} = \frac{1}{2}\left(1 + \frac{2k_j h}{\sinh 2k_j h}\right)\frac{\omega_j}{k_j} \tag{9}$$

where $a_j = \sqrt{2S_{f,j}}$ is the wave amplitude.

[21] Assuming that waves of all frequency components within a spectrum propagate in the same direction the one-dimensional wave energy equation [*Lowe et al.*, 2005] can be applied to estimate the rate of energy dissipation caused by friction ϵ_f per unit area:

$$\frac{\Delta F}{\Delta r} = -\epsilon_f \tag{10}$$

$$\Delta r = \Delta x \cos(\alpha - \beta) \tag{11}$$

where Δr is the projected distance between stations at which energy flux is known. *Lowe et al.* [2005] derived Δr from the measured distance Δx between stations and the wave angle to account for the angle between the direct line connecting the stations α and the direction of wave propagation β.

[22] An original model for ϵ_f was developed for monochromatic waves [*Jonsson*, 1966]. Based on this model, *Madsen* [1994] developed a weighted-average approach which places more weight on the frequency components that contain most wave energy. This approach yields representative parameters to extend the monochromatic models to spectral wave conditions. Following this approach, the representative maximum near-bed horizontal orbital velocity $u_{b,r}$ is defined as:

$$u_{b,r} = \sqrt{\sum_{j=1}^{M} u_{b,j}^2} \tag{12}$$

where $u_{b,j} = a_j\,\omega_j/\sinh k_j h$ is the velocity corresponding to the jth frequency component. Furthermore, *Madsen* [1994] presented a model that derived ϵ_f for a given frequency, j, from the maximum near bed horizontal orbital velocity, $u_{b,j}$, using the energy dissipation factor $f_{e,j}$:

$$\epsilon_{f,j} = \frac{1}{4}\rho f_{e,j} u_{b,r} u_{b,j}^2 \tag{13}$$

Following his weighted approach a representative energy dissipation factor $f_{e,r}$ can be estimated [*Lowe et al.*, 2005]:

$$f_{e,r} = \frac{\sum_{j=1}^{M} f_{e,j} u_{b,j}^2}{\sum_{j=1}^{M} u_{b,j}^2} \tag{14}$$

The energy dissipation factor gives an estimate of how the whole sea grass meadow affects energy dissipation of the entire wavefield and is likely to change throughout the growth cycle or spatially within a meadow. An alternative method for computing ϵ_f was derived by *Dalrymple et al.* [1984] who used the drag coefficient C_D to describe the drag individual sea grass leaves induce on the flow:

$$\epsilon_f = \frac{2}{3\pi}\rho C_D b N \left(\frac{kg}{2\omega}\right)^3 \frac{\sinh^3 ks + 3\sinh ks}{3k\cosh^3 kh} H^3 \tag{15}$$

where b is the leaf width normal to the flow, N is the number of leaves per m^2 and s is the canopy height. This equation accounts for seasonal and spatial changes of the meadow through the plant parameters b, N and s, and therefore implies that C_D is plant specific. The expression assumes rigid vegetation and that the drag coefficient accounts for the horizontal movement of the vegetation [*Dalrymple et al.*, 1984; *Méndez and Losada*, 2004]. While this assumption is a simplification of reality, where sea grass sways with the orbital water motion under waves, *Bradley and Houser* [2009] showed that it is a reasonable first approximation if the plant motion is not known.

4. Results

4.1. Sea Grass Variation

[23] Sea grass growth was strongly seasonal over the 13 month period. Shoot densities (Figure 3a) showed a distinct variation over the growth cycle with maximum shoot densities in summer and minimum values in winter. The average density was 1,980 ± 488 shoots/m^2 (±standard deviation) with a minimum of 625 ± 225 shoots/m^2 in February and a maximum of 4,636 ± 858 shoots/m^2 in August. Leaf lengths (Figure 3b) showed low values in February and March, but almost constant values of 12–16 cm throughout the rest of the year with an annual average of 13 ± 3 cm. Mean values exceeded 16 cm only in October 2008. This value is based on a smaller sample population which may have led to an overestimation of the leaf length. The observed values for shoot density and leaf length are low compared to values observed in the Mediterranean (up to 22,000 shoots/m^2 and 45 cm leaf length [*Curiel et al.*, 1996; *Sfriso and Ghetti*, 1998]). But they agree well with observations made in similar climatic conditions (the Wadden Sea) where maximum shoot densities of 2,000–4,900 shoots/m^2 and leaf lengths of 6–20 cm have been observed [*Schanz and Asmus*, 2003;

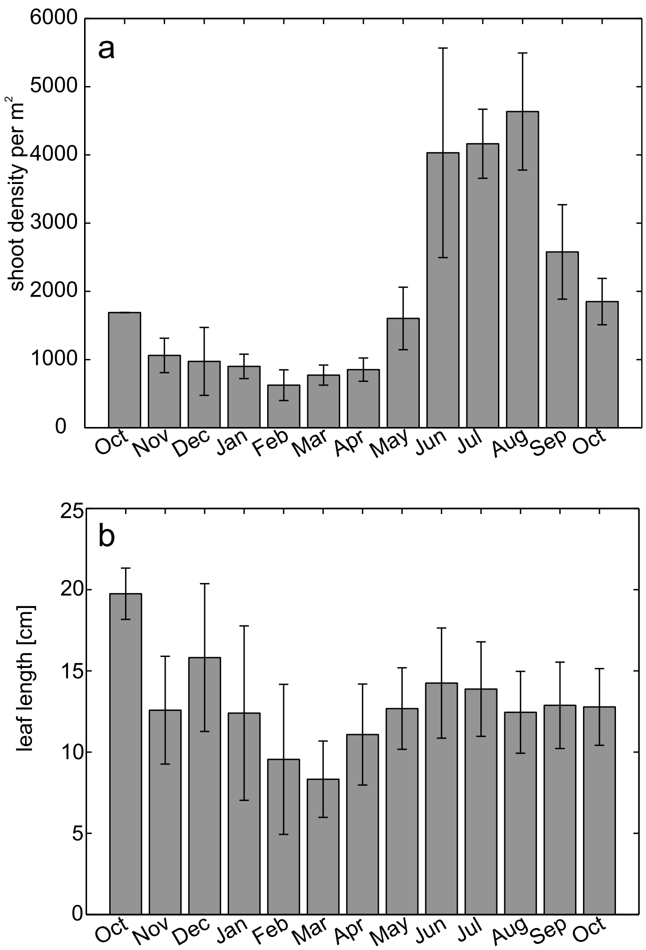

Figure 3. (a) Shoot density per m^2 and (b) leaf length of *Zostera noltii* in Ryde over the 13 month period of monitoring. Uncertainties are expressed by the standard error.

Pasche and Deußfeld, 2003]. This indicates that the *Zostera noltii* meadow in Ryde is well developed and healthy and appears to be representative of meadows at similar latitudes.

4.2. Wave and Tidal Conditions

[24] The tidal flow showed a progressive wave for all deployments with maximum values (~0.3 ms^{-1}) during high and low water and generally lower flow velocities closer to shore. The main flow was in an east-west direction and hence nearly perpendicular to the instrumented transect (Figure 4). While its influence on present waves is consequently negligible [*Madsen*, 1994], the current is likely to affect the sea grass. Sea grass will bend in the presence of a current [*Backhaus and Verduin*, 2008; *Fonseca and Koehl*, 2006] and therefore change its canopy height and orientation relative to wave advance with changing flow velocities and direction. As a tidal current was present during all deployments, it was not included in the scope of this study.

[25] During all deployments, wind waves were generated by northwesterly winds which caused part of the waves to travel along the instrumented transect (Figure 5). Intervals with waves traveling in an east-west direction (±45°) were excluded from analysis to ensure that waves which encountered possible interference from the adjacent pier were not considered. Spectral analysis (equation (1)) was used to compute wave spectra for all intervals and analyses of wave spectra showed that 90% of the energy was contained in the frequency range 0–1 Hz for the majority of the spectra (>90%). Consequently, only frequencies up to 1 Hz were considered for analysis. The spectra (Figure 5) show that wind waves for all deployments occurred in a similar frequency range. Energy dissipation took place across all frequency bands and was most pronounced in July. In October 2008 an increase in energy density along the transect was observed which could not sufficiently be explained with known sources of reflection and refraction. The October 2008 data was therefore excluded from further analysis. Significant

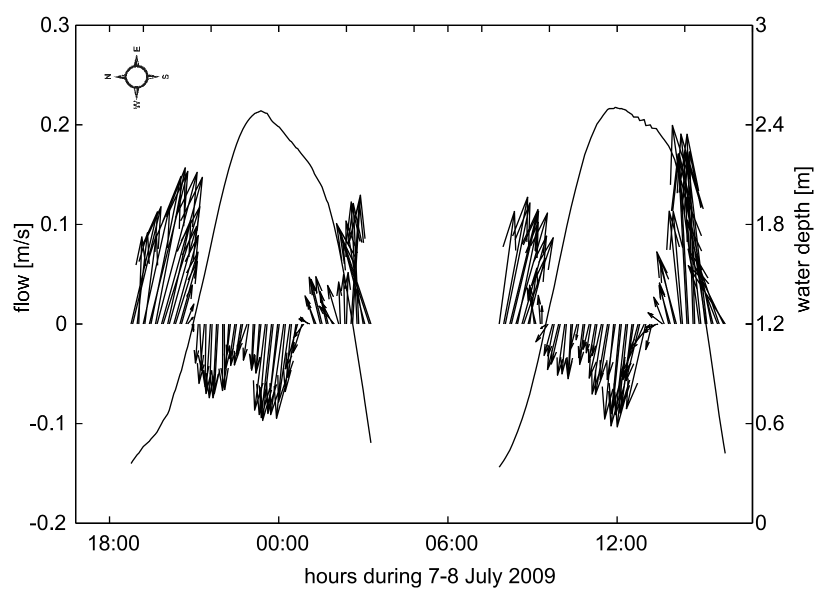

Figure 4. Representative example of tidal flow conditions at station 5 in July 2009. The solid line represents the tidal elevation.

wave height (equation (4)) was calculated from these spectra and maximum wave heights varied from 13 cm in October 2009 to 18 cm in July (Table 1).

[26] Boat wakes were clearly visible in time series during calm conditions and differed significantly from wind waves (Figure 6). Those time series were used to determine the boat wake's frequency (0.1 Hz) and consequently to separate boat wakes from wind waves in the spectra by splitting them into two frequency ranges: f = 0–0.2 Hz for boat wakes and f = 0.2–1 Hz for wind waves.

4.3. Wave Attenuation

[27] As wave energy is directly related to wave height (equation (8)), change in wave height between two stations can be used to compare energy dissipation between deployments once shoaling had been removed. Shoaling coefficients ranged from 1 to 1.05, leading to a maximum increase in wave height of 5% between consecutive stations. Time series of H_s for each deployment (Figure 7) show that wave heights reduce along the transect in small water depths ($h \lesssim 1$ m), while a change in wave height at higher water depths can only be observed in July and October 2009. To explore the difference in wave height reduction between deployments, wave height evolution along the transect for water depths <1 m was examined (Figure 8; see also Table 2). PDCR stations only were used to exclude inaccuracies caused by comparison of different instrument types. Reduction in wave height was greatest in July, when sea grass density was high (4,164 ± 506 shoots/m^2). With a reduction of up to 20% between consecutive stations, the observed wave height reduction was four times higher than the effect of shoaling (<5%), indicating that the sea grass has an effect on wave height reduction. For all other deployments wave height reduction was less than 10% and therefore similar to the effect of shoaling. Moreover, the data alternate around a value of approximately 1 and hence the data show no significant wave attenuation. Values at stations 4 and 6 of the February, May and October 2009 deployments show an increase of wave height of up to 15% compared to values at station 2. While this percentage appears high, absolute values show that the increase is <0.5 cm in all cases and can therefore be neglected based on instrument accuracy.

[28] Based on the observed reduction in wave height the energy dissipation factor $f_{e,r}$ was computed from the wave spectra using equations (10) to (14). To satisfy the condition of equation (10), only intervals with a wave spread of <10° were used. Although Δr in equation (10) accounts for the angle between the transect and wave direction, it was decided to restrict data to intervals where the angle was <20°. At a larger angle, waves cannot be considered to be traveling along the transect and therefore would not give information about wave attenuation between stations.

[29] The site was exposed to wind waves and boat wakes which could be distinguished by the difference in wave period (Figure 6). This was used to separate the two wave types in the wave spectra and to investigate whether waves of different frequencies are attenuated differently. For wind waves, $f_{e,r}$ was constant throughout the year (ANOVA, F = 0.14, p = 0.97) and similar to values for boat wakes. The summer mean ($f_{e,r}$ = 0.17 ± 0.19) of boat wake values is an order of magnitude higher than for the other deployments (Table 3).

[30] Figure 9 shows $f_{e,r}$ for each shore ward station. For wind waves (Figures 9a–9d), values do not differ along the transect, but are distributed around the mean value. For boat wakes a similar behavior can be observed during autumn, winter and spring, resulting in similar mean values to wind waves. In summer, however, a decrease of $f_{e,r}$ toward the shore was observed (Figures 9e–9h).

[31] While a difference in $f_{e,r}$ can be observed with varying sea grass coverage and vitality, it is also dependent on the maximum near-bed horizontal orbital velocity (equations (13) and (14)) and the relationship to wave Reynolds number ($Re = u_{b,r}^2/(\omega\nu)$, ω = wave angular frequency and ν = kinematic viscosity) has been suggested by *Iwagaki and Kakinuma* [1967]. Figure 10 shows the relationship between $f_{e,r}$ and Re for all deployments separated into boat wakes and wind waves.

[32] The majority of values are above the theoretical relationship for laminar conditions and hence are fully turbulent. It has been observed for rough turbulent conditions that the wave friction factor f_w is independent of Reynolds number and solely depends on the relative roughness $u_b/\omega k_N$ where k_N is the equivalent Nikuradse roughness [*Kamphuis*, 1975]. Wave friction factor and energy dissipation factor are linked through the phase lag φ between bottom shear stress and wave orbital velocity

$$f_{e,r} = f_w \cos\varphi \tag{16}$$

$$\varphi = 33 - 6\log\frac{u_b}{\omega k_N} \tag{17}$$

It can therefore be assumed that a similar relationship with relative roughness exists for $f_{e,r}$ [*Madsen*, 1994]. Several formulas have been proposed to describe the relationship between friction factor and relative roughness: The one by *Nielsen* [1992] is the most widely used:

$$f_w = \exp\left[5.5\left(\frac{u_b}{\omega k_N}\right)^{-0.2} - 6.3\right]. \tag{18}$$

[33] Using this relationship between energy dissipation factor and relative roughness, an attempt was made to estimate k_N. The equivalent Nikuradse roughness was initially defined to evaluate bedforms as roughness elements and describe bed roughness through a single parameter [*Nielsen*, 1992]. However, the application of this parameter to flexible vegetation is unproven.

[34] *Madsen* [1994] proposed an alternative to equation (18) in his spectral model which includes a parameter C_μ to account for the effect of an underlying current. While a variable current existed during the present experiments (Figure 4), it was chosen to neglect its effect on f_w for several reasons. While a current is likely to cause bending of the flexible vegetation leaves, it is not known in detail how the current affects sea grass. Additionally, experiments over fixed beds showed that k_N is bed specific and is not affected by changing hydrodynamic conditions [*Mathisen and Madsen*, 1999]. Equation (18) should therefore yield a good first approximation, especially as values of C_μ are generally close to unity [*Madsen*, 1994].

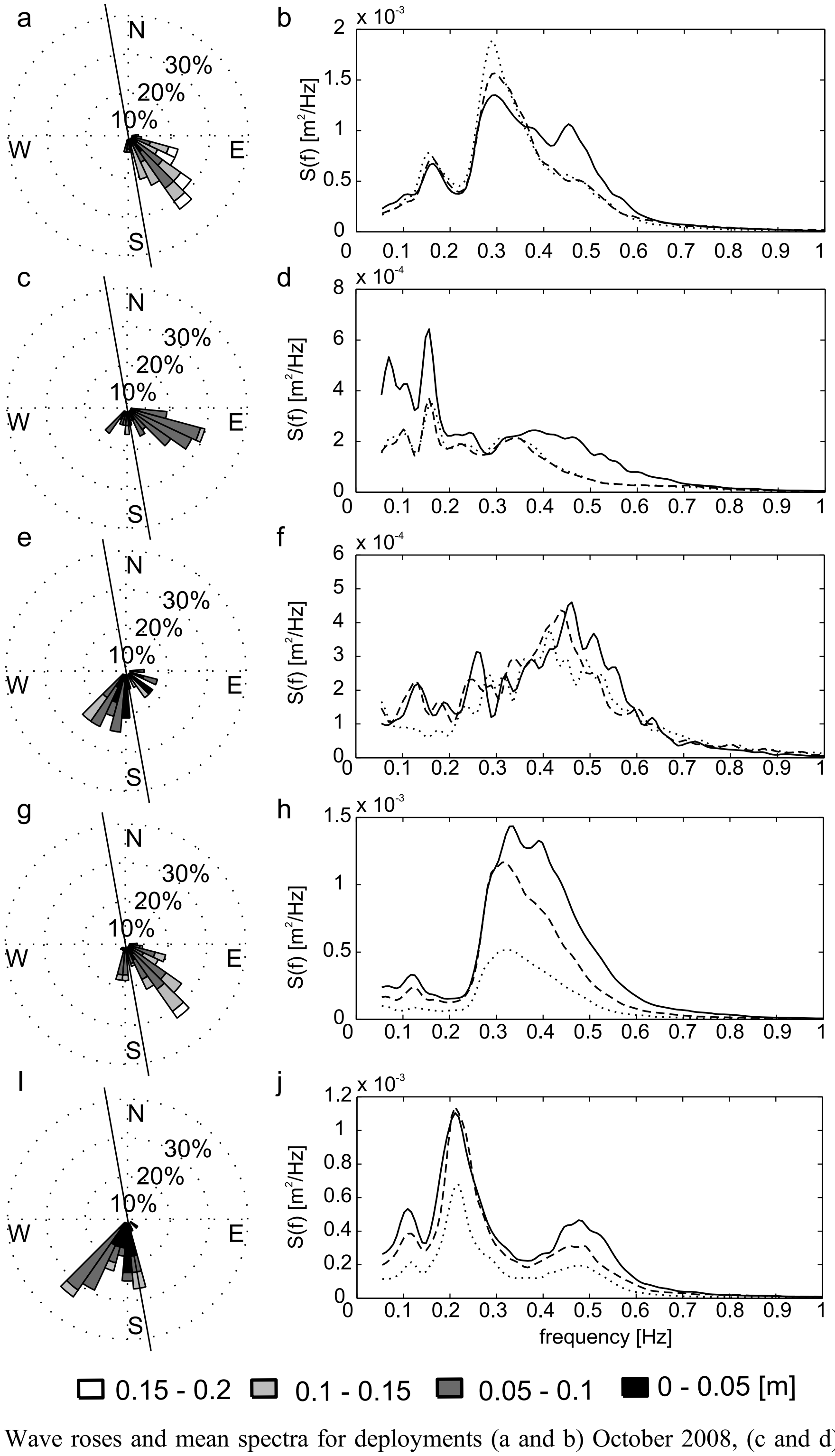

Figure 5. Wave roses and mean spectra for deployments (a and b) October 2008, (c and d) February, (e and f) May, (g and h) July, and (i and j) October 2009 after removing waves from easterly directions. The solid line in the wave roses represents the transect angle. In the spectra, the solid line represents the outermost station, the dashed line represents station 3 or 4 (depending on availability), and the dotted line represents the innermost station.

[35] Equation (16), in conjunction with equations (17) and (18), did not show a significant trend (Table 4). By contrast, the values appeared to alternate around a common mean and any change throughout the year seemed to fall within the natural variability. The mean value for this study was 0.17 m which is similar to roughnesses found for rough and rippled beds. *Mathisen and Madsen* [1996a, 1996b, 1999] estimated bed roughnesses of 0.14–0.28 m over evenly spaced, tri-

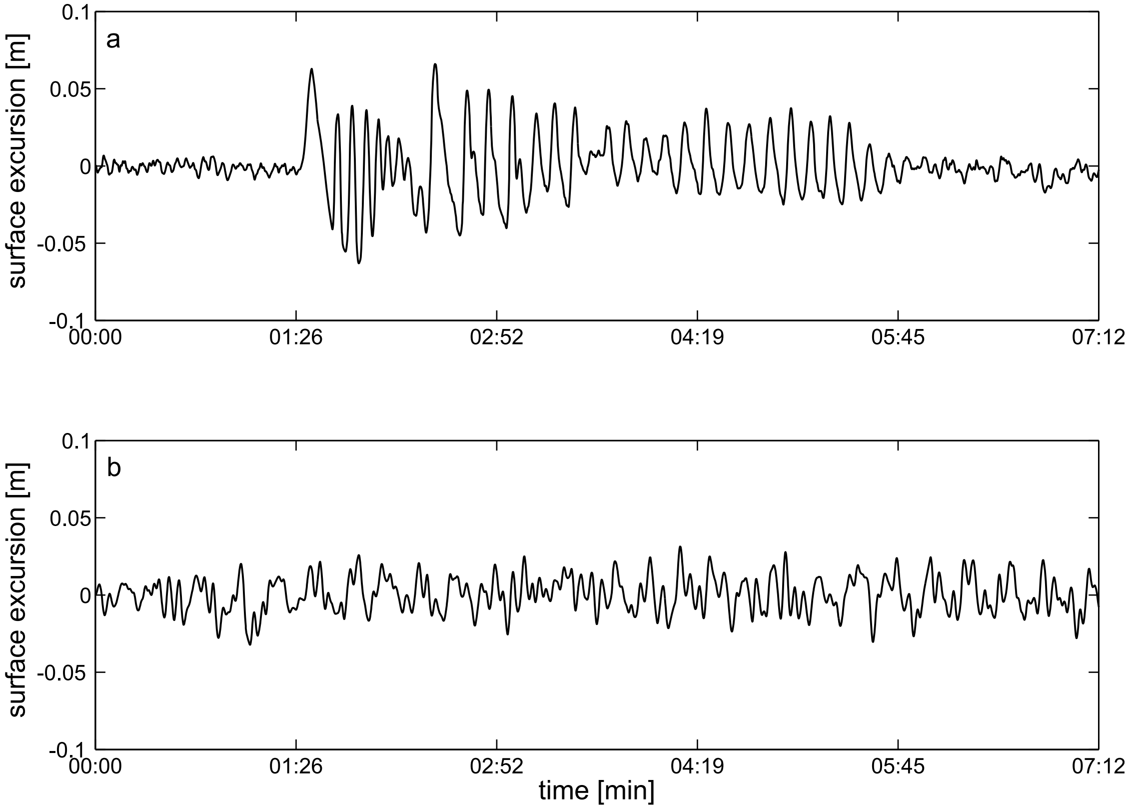

Figure 6. Time series of representative (a) boat wake generated by a ferry leaving from the pier head and (b) wind wave conditions.

angular bars during laboratory experiments and a field study found k_N = 0.16 m for a coral reef [*Lowe et al.*, 2005]. *Iwagaki and Kakinuma* [1967] carried out measurements over rippled sand of grain sizes similar to those grain sizes found in Ryde; thus from their data k_N = 0.13 m was derived.

[36] Because the energy dissipation factor is dependent on the seasonality of sea grass characteristics, it is not appropriate to compare the wave attenuation effect between different species. A parameter more suitable for such a comparison is the drag coefficient C_D (equation (15)). A

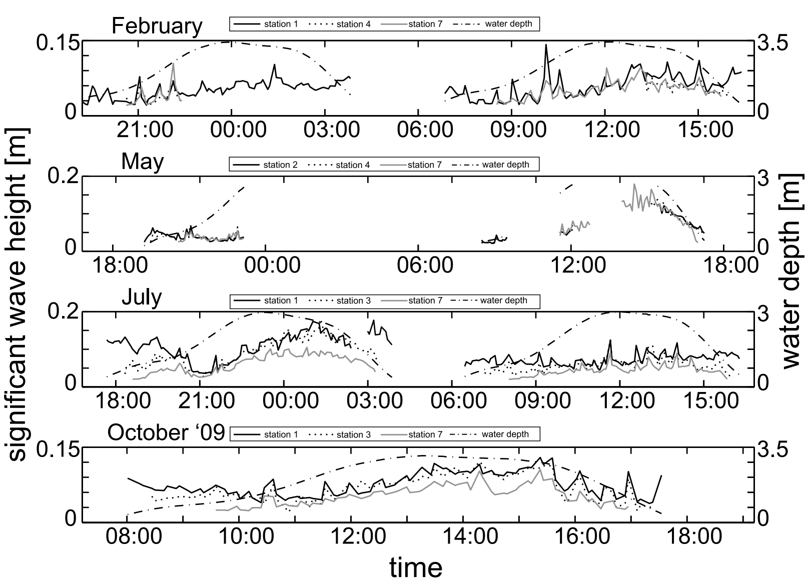

Figure 7. Time series of significant wave height for each deployment. Some stations have been omitted for clarity. The dash-dot line represents water depth.

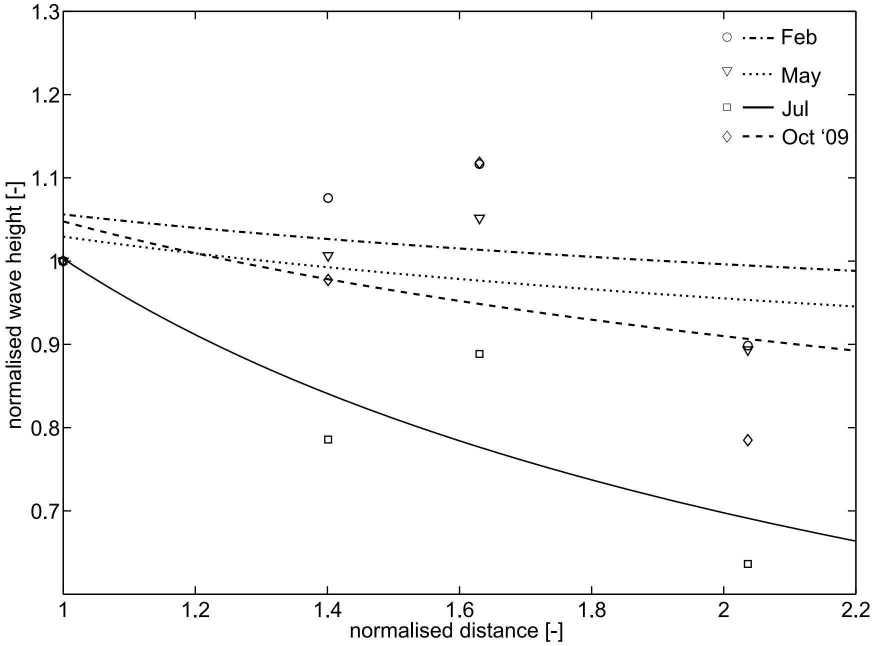

Figure 8. Mean normalized significant wave height in water depths <1 m for all deployments and corresponding regression lines. See Table 2 for regression parameters.

comparison of the time averaged drag coefficient shows that C_D behaves similar across frequencies for all deployments (Figure 11). For frequencies <0.4 Hz the values alternate around a constant value of 1.67 ± 0.07 before they increase with increasing frequency. The latter is in agreement with observations by *Bradley and Houser* [2009] who found an increase of C_D with increasing frequency for f > 0.4 Hz in a *Thalassia testudinum* bed. They also observed a reduction in C_D at f = 0.38 Hz and suggested that this can be attributed to the relative motion of the sea grass which is not uniform across frequencies. While in this study a slight increase at 0.2 Hz and a decrease at 0.45 Hz could be observed in July, this variation was not significantly different from the other deployments (ANOVA, F = 1.19, p = 0.31). The dependence of C_D on sea grass motion as suggested by *Bradley and Houser* [2009] could therefore not be found during the present study. This could be due to the presence of an underlying current for parts of the tidal cycle, which would affect the swaying motion of the sea grass. No data are available on the relative motion of *Z. noltii* in Ryde and the above hypothesis could therefore not be addressed within this study. However, the results show that there is no significant difference in C_D for boat wakes and wind waves and values from both wave types can be evaluated together.

[37] In previous studies a relationship of the representative drag coefficient with the vegetation Reynolds number ($Re_v = bu_b/\nu$) has been found [*Kobayashi et al.*, 1993; *Méndez et al.*, 1999; *Bradley and Houser*, 2009]. The vegetation Reynolds number is considered more suitable in this case than the wave Reynolds number, because, like C_D, it includes a vegetation parameter rather than wave parameters only. A relationship of C_D with Re_v can be observed with an increase at low Reynolds numbers and approaching a constant value for $Re_v \gtrsim 600$ (Figure 12). Previous studies proposed a relationship of the from $C_D = a + (b/Re_v)^c$ [*Kobayashi et al.*, 1993; *Méndez et al.*, 1999; *Bradley and Houser*, 2009] which yielded for the present data ($R^2 = 0.37$, n = 46):

$$C_D = 0.34 + \left(\frac{97.9}{Re_v}\right)^{4.02}. \tag{19}$$

[38] The scatter is caused by the varying hydrodynamic conditions throughout the study; especially wave height affects C_D as it appears in equation (15) with a power of 3. If

Table 2. Statistical Values for the Relationship of H_s With Water Depth of the Form $H_s/H_{s0} = a(x/x_0)^b$[a]

	a	b	R^2	H_{s0} [cm]
February	1.06	−0.08	0.07	4.5
May	1.03	−0.11	0.23	5.1
July	1.01	−0.52	0.74	5.9
October 2009	1.05	−0.20	0.19	3.4

[a]Here the index 0 denotes values at the outermost station, and x is the station's distance from a reference point offshore of station 1.

Table 3. Mean Values of $f_{e,r}$ for Wind Waves (f = 0.2–1 Hz) and Boat Wakes (f = 0–0.2 Hz) for All Deployments[a]

	Wind Waves	Boat Wakes
February	0.07 ± 0.09	0.08 ± 0.1
May	0.06 ± 0.04	0.05 ± 0.03
July	0.08 ± 0.07	0.17 ± 0.19
October 2009	0.08 ± 0.05	0.09 ± 0.04

[a]Uncertainties are expressed as the standard deviation of the scatter.

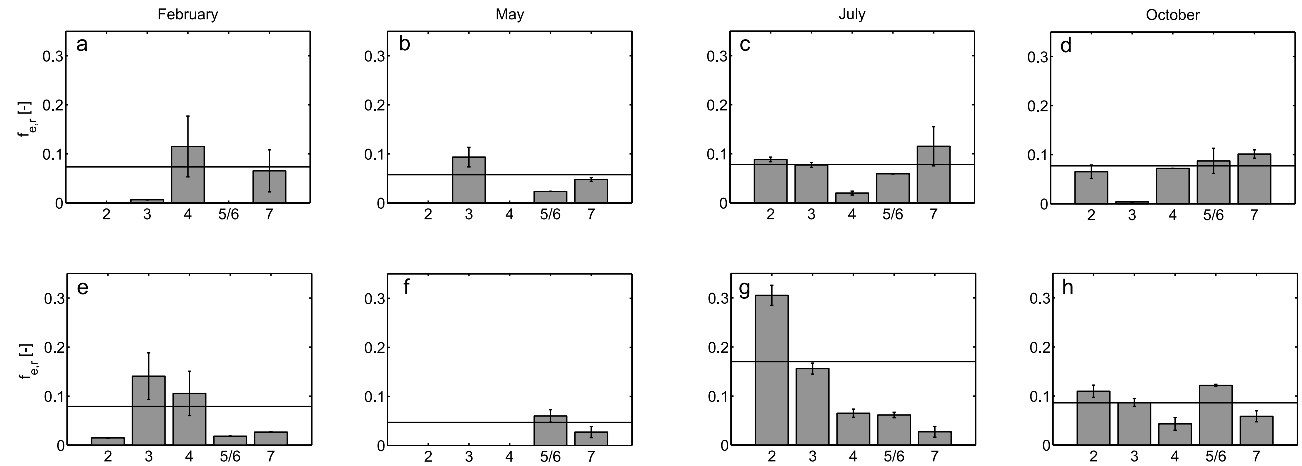

Figure 9. Comparison of $f_{e,r}$ between stations for each deployment for (a-d) wind waves and (e-h) boat wakes. The solid line indicates the respective mean value, and uncertainties are represented by the standard error.

only data with $H_s \geq 0.1$ m is considered, a good fit ($R^2 = 0.96$, n = 14) of the form:

$$C_D = 0.06 + \left(\frac{153}{Re_v}\right)^{1.45} \tag{20}$$

can be achieved (Figure 12) and values for $H_s < 0.1$ m scatter around this fit.

5. Discussion

[39] It is widely accepted that sea grass attenuates waves [*Fonseca*, 1996; *Ward et al.*, 1984; *Newell and Koch*, 2004; *Koch et al.*, 2006, 2009] and although laboratory studies showed that wave height reduction responds nonlinearly to vegetation traits such as density and canopy height as well as distance into the meadow [*Fonseca and Cahalan*, 1992; *Bouma et al.*, 2010; *Méndez et al.*, 1999; *Kobayashi et al.*, 1993] field studies to support these observations are still scarce [*Bradley and Houser*, 2009; *Newell and Koch*, 2004; *Bouma et al.*, 2005]. The present study investigated wave attenuation over a *Zostera noltii* meadow at four different stages during the growth cycle and found a dependence of energy dissipation on sea grass traits as well as hydrodynamics. The *Zostera noltii* meadow in Ryde was exposed to natural wind waves and boat wakes which allowed an initial

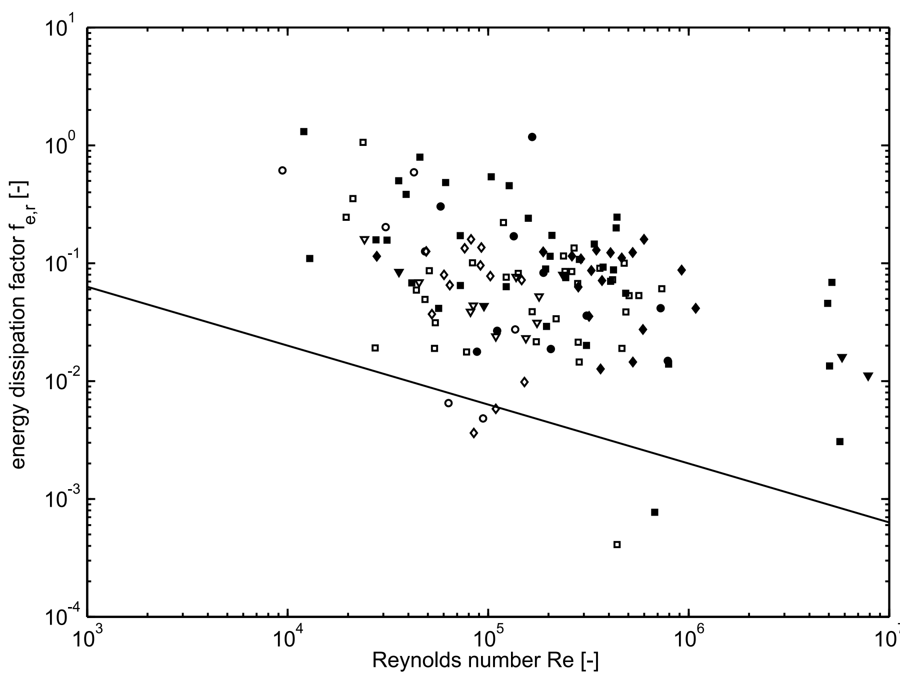

Figure 10. Relationship of $f_{e,r}$ and wave Reynolds number Re for all deployments. Filled symbols, boat wakes; open symbols, wind waves; circles, February; triangles, May; squares, July; diamonds, October 2009. The solid line represents the relationship to Re under conditions of laminar flow $f_{e,r} = 2/\sqrt{Re}$.

Table 4. Average Energy Dissipation Factors $f_{e,r}$ and Bed Roughnesses k_N for All Deployments[a]

	$f_{e,r}$	k_N
February	0.07 ± 0.1	0.14 ± 0.07
May	0.02 ± 0.02	0.17 ± 0.04
July	0.06 ± 0.05	0.14 ± 0.06
October 2009	0.05 ± 0.03	0.21 ± 0.15

[a]Uncertainties are expressed as the standard deviation of the scatter.

evaluation of the effect of hydrodynamic forcing on its wave attenuating capacity. However, no storm conditions were encountered during measurements and the present data set is thus not sufficient to reliably predict the effect of *Zostera noltii* on all occurring wave conditions. Hydrodynamic forcing is likely to be higher (i.e., storms) in winter when shoot densities are low and *Zostera noltii* may therefore play a limited role inshore protection by wave attenuation.

[40] The representative energy dissipation factor $f_{e,r}$ decreased toward the shore for boat wakes in July while it remained constant across the sand flat for all other deployments and hydrodynamic conditions. This difference in behavior could be due to the sea grass presence. While sea grass is present during all other deployments, density in July is at least twice that of other deployments. *Newell and Koch* [2004] found that a minimum shoot density was required for *Ruppia maritima* to have a measurable effect on wave attenuation. This might also be true for *Zostera noltii*: The data suggest that the threshold lies between approximately 2,000 and 4,000 shoots/m^2. Above this threshold, the sea grass changes the wave attenuating function of the bed, causing higher friction at the outer stations and therefore attenuating the waves more effectively. Similar behavior has been found in salt marsh [*Möller et al.*, 1999; *Bouma et al.*, 2005] and although it is not necessarily beneficial for the plants that cause wave attenuation, it will create more suitable conditions for other plants within the meadow and can therefore be considered as a division of labor within the ecosystem [*Bouma et al.*, 2005]. While sea grass is morphologically very different from salt marsh vegetation, and its flexible leaves bend a lot more under flows, an exponential decay of wave attenuation has been observed in *Thalassia testudinum* [*Bradley and Houser*, 2009] and is therefore likely at high densities for *Z. noltii* as well.

[41] The effect of density and wave frequency did not reflect in the values for bed roughness k_N despite its relationship to $f_{e,r}$ described in equation (16), in conjunction with equations (17) and (18). Values derived for all deployments did not differ significantly (Table 4) and fell within the range of roughnesses estimated for rough and rippled beds [*Mathisen and Madsen*, 1996a; *Lowe et al.*, 2005; *Iwagaki and Kakinuma*, 1967; *Mathisen and Madsen*, 1996b, 1999]. That the values do not correlate with sea grass growth may be due to the range of water depths covered in this study. Figure 7 shows wave height reduction did not take place in water deeper than 1 m. The majority of data that fit the quality criteria wave spread <10° and $\alpha - \beta < 20°$ (in equation (11)) to calculate $f_{e,r}$ and k_N, however, came from depths >1 m. It could be possible that the effect of *Zostera noltii* on wave attenuation in such water depths is very small and differences

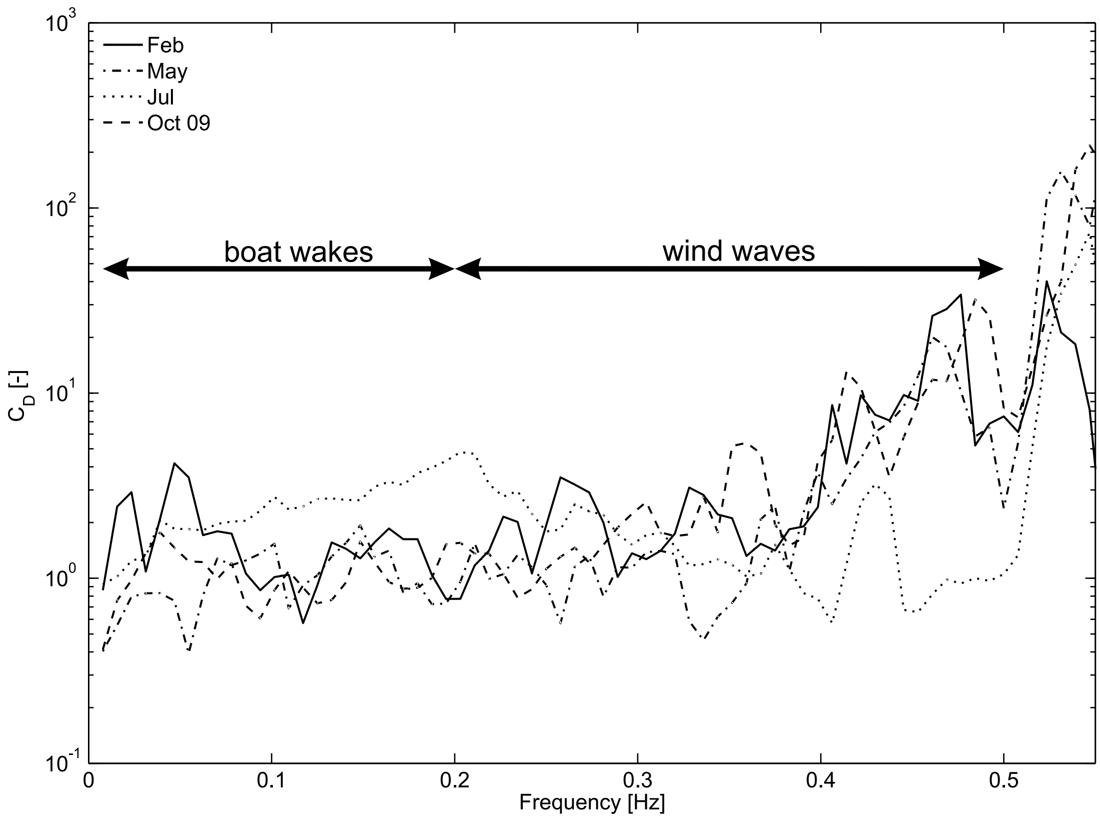

Figure 11. Time and spatial averaged drag coefficient by wave frequency.

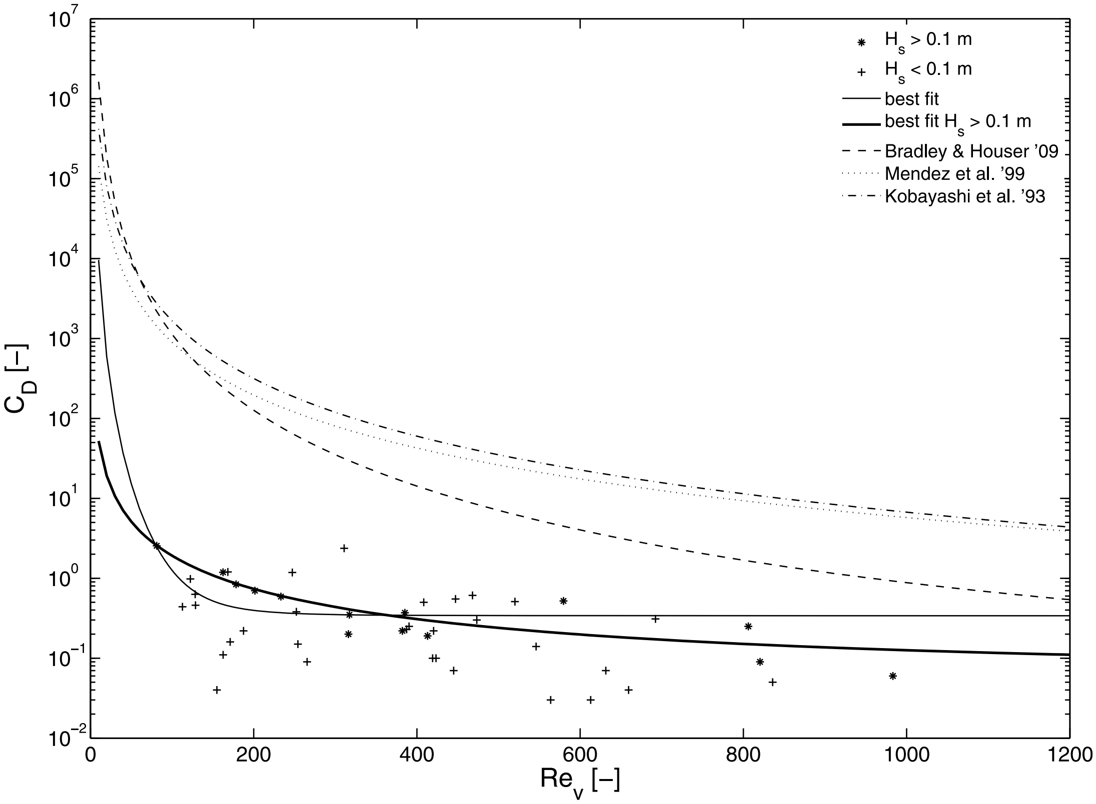

Figure 12. Relationship between C_D and vegetation Reynolds number Re_v and the best fit for all data and H_s > 0.1 m. Also shown are the best fit lines for *Bradley and Houser* [2009] ($C_D = 0.1 + (925/Re_v)^{3.16}$), *Méndez et al.* [1999] ($C_D = 0.08 + (2200/Re_v)^{2.2}$), and *Kobayashi et al.* [1993] ($C_D = 0.08 + (2200/Re_v)^{2.4}$).

between deployments could therefore not be detected in the mean values for $f_{e,r}$ and k_N (Table 4). Another possible reason why the estimated values do not correlate with sea grass growth could lie within the method itself. The method used within this paper is based on linear wave theory which may oversimplify the wave conditions encountered in Ryde. Moreover, *Madsen*'s [1994] relationship between friction factor and bed roughness is based on the assumption that k_N is independent of ambient hydrodynamic conditions. This assumption has been validated for fixed beds in laboratory studies [*Mathisen and Madsen*, 1999], but may not be valid for flexible vegetation. Vegetation moves with the orbital motions under waves; it changes its shape constantly and hence its roughness is not likely to remain constant. If this is the case, *Madsen*'s [1994] method may not be suitable to determine the bed roughness and therefore wave friction associated with a vegetated bed. Another source of inaccuracy may be the assumption that wave reflection by the sea grass is negligible and wave energy flux is traveling onshore only. Laboratory studies have shown that reflection can occur along the edges of vegetation meadows and can generate a modulation in wave force along the vegetation field [*Méndez and Losada*, 2004; *Méndez et al.*, 1999]. To reduce the impact of this effect on the present analysis, all instruments were placed inside the meadow, at least 100 m away from its leading and trailing edge. Reflection from the top of the vegetation canopy may have occurred, however, instrument spacing in the present study did not allow calibration of such reflection [*Möller et al.*, 1999]. Moreover, reflection by vegetation canopies has been found to be insignificantly small in laboratory and numerical studies [*Li and Zhang*, 2010; *Méndez and Losada*, 2004; *Méndez et al.*, 1999] and it was therefore decided to neglect its impact on propagation of wave energy flux (equation (10)) in the present study.

[42] An alternative parameter to describe energy dissipation is the drag coefficient C_D which is independent of the seasonality of sea grass density and leaf length, but shows a relationship with hydrodynamics in the form of the vegetation Reynolds number Re_v (Figure 12). Figure 12 also shows the curves derived by *Kobayashi et al.* [1993], *Méndez et al.* [1999] and *Bradley and Houser* [2009] respectively. *Kobayashi et al.* [1993] developed a model for wave damping of monochromatic waves under the assumption that vegetation can be represented by fixed cylindrical elements. They applied their model to data obtained by *Asano et al.* [1988] who carried out laboratory experiments on artificial kelp. *Méndez et al.* [1999] extended the model to random waves and also used the data from *Asano et al.* [1988] to validate their model. The resulting relationship gives slightly lower values than the one by *Kobayashi et al.* [1993]. *Bradley and Houser* [2009] applied equation (15) to field data obtained in a *T. testudinum* meadow and derived the relationship shown in Figure 12.

[43] From the empirical fits, a difference between species can be seen and it is possible to deduce a dependence of C_D on vegetation stiffness. Under the assumption that poly-

propylene represents the kelp's plant stiffness well during *Asano et al.*'s [1988] laboratory experiments, they will have been stiffer than *T. testudinum* or *Z. noltii.* This would lead to a higher drag coefficient for a given value of Re_v. The difference between *T. testudinum* and *Z. noltii* can be explained in a similar fashion, because *T. testudinum* leaves are less flexible than *Z. noltii* leaves [*Kuo and Den Hartog*, 2006].

6. Conclusions

[44] The results show that *Zostera noltii* has an effect on wave attenuation which varies seasonally with shoot density. However, a minimum density was required before attenuation can be observed. The existence of such a threshold suggests a nonlinear relationship between the two parameters. Moreover, the density threshold varies with hydrodynamics; the higher the wave period is, the lower is the required density to initiate wave attenuation.

[45] Once the threshold density is exceeded, a change in energy dissipation with distance from the shore can be observed, but the present data set is not sufficient to establish whether this change in linear or nonlinear. A clear nonlinear relationship has been found, however, for the drag coefficient C_D. It describes the drag per unit plant area and is therefore independent of seasonal parameters such as height and density. Consequently, it can be applied all year round, but it changes with hydrodynamic conditions. While a strong relationship with Reynolds number was found for waves with a wave height ≥0.1 m, scatter increased when waves with a lower wave height were considered.

[46] Overall, the data indicate that wave attenuation over vegetation does not only depend on plant characteristics, but also on the hydrodynamics that act on the plants. While it has been recognized that sea grass attenuates waves [*Fonseca and Cahalan*, 1992; *Newell and Koch*, 2004; *Bouma et al.*, 2010], the rate of wave attenuation varies between species and each species needs to be evaluated individually [*James and Barko*, 2000]. The fact that a dependence on plant characteristics as well as hydrodynamics can be observed in a relatively small species such as *Zostera noltii* suggests it may occur in larger species as well. However, detailed studies on other sea grass species are still rare. Nevertheless, the combined interaction of plant characteristics and hydrodynamics adds to the complexity of estimating the economic value of sea grass meadows and describing the effect plant attributes have on wave attenuation is only the beginning.

Notation

- a wave amplitude
- b leaf width
- C_D drag coefficient
- C_g group velocity
- C_μ current parameter in *Madsen*'s [1994] model
- CD Chart Datum
- CS cross-spectrum
- D wave direction
- E wave energy density
- f_e energy dissipation factor
- f_w wave friction factor
- F wave energy flux
- g gravitational acceleration
- h water depth
- H_s significant wave height
- H_{rms} root-mean-square wave height
- k wave number
- k_N equivalent Nikuradse roughness
- K_s shoaling coefficient
- L wavelength
- M Number of discrete frequency components
- N number of leaves per m^2
- Re wave Reynolds number
- Re_v vegetation Reynolds number
- s canopy height
- spr wave spreading
- S_f energy density spectrum
- S_{pr} pressure spectrum
- T wave period
- u_b near-bed horizontal orbital velocity
- x distance of station from a reference point offshore of station 1
- z vertical distance measured up from seabed
- α angle of the instrumented transect
- β direction of wave propagation
- γ critical breaking parameter
- Δf_b frequency bandwidth
- Δr projected distance between stations
- Δx measured distance between stations
- ϵ_f rate of frictional dissipation
- ρ density of water
- ν kinematic viscosity
- φ phase difference between bottom shear stress and wave orbital velocity
- ω radian wave period

Subscripts

- 0 outermost station
- j frequency component j
- n number of the shore ward station
- p pressure
- r representative parameter
- u East component of velocity
- v North component of velocity

[47] **Acknowledgments.** The project was funded with the help of the German Academic Exchange Service, IMarEST and the Solent Forum. The authors kindly acknowledge the use of MatLab code for spectral analysis provided by U. Neumeier. Additionally, the authors would like to thank Wightlink Limited for the use of their facilities during field work. Special thanks also to Stephen Duffy for his invaluable help during field deployments and to numerous members of the NOC community for their help in the field. The authors would also like to thank Ian Townend for input during data analysis and two anonymous reviewers whose comments improved the manuscript.

References

Asano, T., S. Tsutsui, and T. Sakai (1988), Wave damping characteristics due to seaweed (in Japanese), in *Proceedings of the 35th Japanese Conference on Coastal Engineering*, pp. 138–142, Jpn. Soc. of Civ. Eng., Tokyo.

Auby, I., and P.-J. Labourg (1996), Seasonal dynamics of *Zostera noltii Hornem.* in the Bay of Arcachon (France), *J. Sea Res.*, *35*(4), 269–277.

Backhaus, J., and J. Verduin (2008), Simulating the interaction of seagrasses with their ambient flow, *Estuarine Coastal Shelf Sci.*, *80*, 563–572.

Barbier, E., et al. (2008), Coastal ecosystem-based management with nonlinear ecologial functions and values, *Science*, *319*, 321–323, doi:10.1126/science.1150349.

Battjes, J. (1974), Surf similarity, in *Proceedings of the 14th Coastal Engineering Conference*, pp. 466–480, Am. Soc. of Civ. Eng., Reston, Va.

Bouma, T., M. De Vries, E. Low, G. Peralta, I. Tánczos, J. van de Koppel, and P. Herman (2005), Trade-offs related to ecosystem engineering: A case study on stiffness of emerging macrophytes, *Ecology*, *86*(8), 2187–2199.

Bouma, T., M. De Vries, and P. Herman (2010), Comparing ecosystem engineering efficiency of 2 plant species with contrasting growth strategies, *Ecology*, *91*(9), 2696–2704.

Bradley, K., and C. Houser (2009), Relative velocity of seagrass blades: Implications for wave attenuation in low-energy environments, *J. Geophys. Res.*, *114*, F01004, doi:10.1029/2007JF000951.

Brun, F., A. Pérez-Pastor, I. Hernández, J. Vergara, and J. Pérez-Lloréns (2006), Shoot organization in the seagrass *Zostera noltii*: Implications for space occupation and plant architecture, *Helgoland Mar. Res.*, *60*, 59–69, doi:10.1007/s10152-005-0017-0.

Ciavola, P. (2005), Sediment resuspension in the lagoon of venice: Short-term observations of natural and anthropogenic processes, *Z. Geomorphol.*, *141*, 1–15.

Curiel, D., A. Bellato, A. Rismondo, and M. Marzocchi (1996), Sexual reproduction of *Zostera noltii Hornemann* in the lagoon of Venice (Italy, north Adriatic), *Aquat. Bot.*, *52*, 313–318.

Dalrymple, R., J. Kirby, and P. Hwang (1984), Wave diffraction due to areas of energy dissipation, *J. Waterw. Port Coastal Ocean Eng.*, *110*(1), 67–79.

Dean, R., and R. Dalrymple (1991), *Water Wave Mechanics for Engineers and Scientists*, Prentice-Hall, Englewood Cliffs, N. J.

Duarte, C., M. Merino, N. Agawin, J. Uri, M. Fortes, M. Gallegos, N. Marbà, and M. Hemminga (1998), Root production and belowground seagrass biomass, *Mar. Ecol. Prog. Ser.*, *171*, 97–108.

Fonseca, M. (1996), The role of seagrasses in nearshore sedimentary processes: a review, in *Estuarine Shores: Evolution, Environments and Human Alterations*, edited by K. Nordstrom and C. Roman, pp. 261–286, John Wiley, Chichester, N. Y.

Fonseca, M., and J. Cahalan (1992), A preliminary evaluation of wave attenuation by four species of seagrass, *Estuarine Coastal Shelf Sci.*, *35*, 565–576.

Fonseca, M., and J. Fisher (1986), A comparison of canopy friction and seagrass movement between four species of seagrass with reference to their ecological restoration, *Mar. Ecol.*, *29*, 15–22.

Fonseca, M., and M. Koehl (2006), Flow in seagrass canopies: The influence of patch width, *Estuarine Coastal Shelf Sci.*, *67*, 1–9.

Garel, E., L. Fernandez, and M. Collins (2008), Sediment resuspension events induced by the wake wash of deep-draft vessels, *Geo Mar. Lett.*, *28*, 205–211.

Gordon, L., and A. Lohrmann (2001), Near-shore Doppler current meter wave spectra, technical report, Nortek, Sandvika, Norway.

Iwagaki, Y., and T. Kakinuma (1967), On the bottom friction factors off five Japanese coasts, *Coastal Eng. Japan*, *10*, 13–22.

James, W., and W. Barko (2000), Sediment resuspension dynamics in canopy- and meadow-forming submersed macrophyte communities, *Rep. ERDC/EL SR-00-8*, 40 pp., Aquat. Plant Control Res. Program, U.S. Army Corps of Eng., Vicksburg, Miss.

Jonsson, I. (1966), Wave boundary layers and friction factors, in *10th Conference on Coastal Engineering*, vol. 1, pp. 127–148, Am. Soc. of Civ. Eng., Reston, Va.

Kamphuis, J. (1975), Friction factor under oscillatory waves, *J. Waterw. Harbors Coastal Eng. Div. Am. Soc. Civ. Eng.*, *101*(WW2), 135–144.

Kobayashi, N., A. Raichle, and T. Asano (1993), Wave attenuation by vegetation, *J. Waterw. Port Coastal Ocean Eng.*, *119*, 30–48.

Koch, E. (2002), Impact of boat-generated waves on seagrass habitat, *J. Coastal Res.*, *37*, 66–74.

Koch, E., J. Ackerman, J. Verduin, and M. van Keulen (2006), Fluid dynamics in seagrass ecology: From molecules to ecosystems, in *Seagrasses: Biology, Ecology and Conservation*, edited by A. Larkum, R. Orth, and C. Duarte, pp. 193–225, Springer, Berlin.

Koch, E., et al. (2009), Non-linearity in ecosystem services: Temporal and spatial variability in coastal protection, *Frontiers Ecol. Environ.*, *7*(1), 29–37, doi:10.1890/080126.

Krogstad, H., S. Barstow, O. Haug, and D. Peters (1998), Directional distributions in wave spectra, in *WAVES'97*, pp. 883–895, Am. Soc. of Civ. Eng., Reston, Va.

Kuo, J., and C. Den Hartog (2006), Seagrass morphology, anatomy, and ultrastructure, in *Seagrasses: Biology, Ecology and Conservation*, edited by A. Larkum, R. Orth, and C. Duarte, pp. 51–87, Springer, Berlin.

Lentz, S., and B. Raubenheimer (1999), Field observations of wave setup, *J. Geophys. Res.*, *104*(C11), 25,867–25,875.

Li, C., and M. Zhang (2010), 3D modelling of hydrodynamics and mixing in a vegetation field under waves, *Comput. Fluids*, *39*(4), 604–614, doi:10.1016/j.compfluid.2009.10.010.

Lowe, R., J. Falter, M. Bandet, G. Pawlak, M. Atkinson, S. Monismith, and J. Koseff (2005), Spectral wave dissipation over a barrier reef, *J. Geophys. Res.*, *110*, C04001, doi:10.1029/2004JC002711.

Lowe, R., J. Falter, J. Koseff, S. Monismith, and M. Atkinson (2007), Spectral wave flow attenuation within submerged canopies: Implications for wave energy dissipation, *J. Geophys. Res.*, *112*, C05018, doi:10.1029/2006JC003605.

Madsen, J., P. Chambers, W. James, E. Koch, and D. Westlake (2001), The interaction between water movement, sediment dynamics and submersed macrophytes, *Hydrobiologia*, *444*, 71–84.

Madsen, O. (1976), Wave climate on the continental margin: Elements of its mathematical description, in *Marine Sediment Transport and Enrivonmental Management*, edited by D. Stanley and D. Swift, pp. 65–87, John Wiley, New York.

Madsen, O. (1994), Spectral wave-current bottom boundary layer flows, in *24th Conference of Coastal Engineering*, edited by B. Edge, pp. 384–398, Am. Soc. of Civ. Eng., Reston, Va.

Magne, R., F. Ardhuin, V. Rey, and T. H. C. Herbers (2005), Topographical scattering of waves: Spectral approach, *J. Waterw. Port Coastal Ocean Eng.*, *131*(6), 311–320, doi:10.1061/(asce)0733-950x(2005)131:6(311).

Manca, E. (2010), Effects of *Posidonia oceanica* seagrass on nearshore waves and wave-induced flows, Ph.D. thesis, University of Southampton, Southampton, U. K.

Mathisen, P., and O. Madsen (1996a), Waves and currents over a fixed rippled bed: 1. Bottom roughness experienced by waves in the presence and absence of currents, *J. Geophys. Res.*, *101*(C7), 16,533–16,542.

Mathisen, P., and O. Madsen (1996b), Waves and currents over a fixed rippled bed: 2. Bottom and apparent roughness experienced by currents in the presence of waves, *J. Geophys. Res.*, *101*(C7), 16,543–16,550.

Mathisen, P., and O. Madsen (1999), Waves and currents over a fixed rippled bed: 3. Bottom and apparent roughness for spectral waves and currents, *J. Geophys. Res.*, *104*(C8), 18,447–18,461.

Méndez, F., and I. Losada (2004), An empirical model to estimate the propagation of random breaking and nonbreaking waves over vegetation fields, *Coastal Eng.*, *51*(2), 103–118, doi:10.1016/j.coasaleng.2003.11.003.

Méndez, F., I. Losada, and M. Losada (1999), Hydrodynamics induced by wind waves in a vegetation field, *J. Geophys. Res.*, *104*(C8), 18,383–18,396.

Möller, I., T. Spencer, J. French, D. Leggett, and M. Dixon (1999), Wave transformation over salt marshes: A field and numerical modelling study from north Norfolk, England, *Estuarine Coastal Shelf Sci.*, *49*, 411–426.

Mullarney, J., and S. Henderson (2010), Wave-forced motion of submerged single-stem vegetation, *J. Geophys. Res.*, *115*, C12061, doi:10.1029/2010JC006448.

Newell, R., and E. Koch (2004), Modeling seagrass density and distribution in response to changes in trubidity stemming from bivalve filtration and seagrass sediment stabilization, *Estuaries*, *27*, 793–806.

Nielsen, P. (1992), *Coastal Bottom Boundary Layers and Sediment Transport*, World Sci., Singapore.

Pasche, E., and N. Deußfeld (2003), Hydro- und Morphodynamik in Seegraswiesen, *Hansa Int. Maritime J.*, pp. 67–73.

Pergent-Martini, C., V. Pasqualini, L. Ferratt, G. Pergent, and C. Fernandez (2005), Seasonal dynamics of *Zostera noltii Hornem.* in two Mediterranean lagoons, *Hydrobiologia*, *543*, 233–243, doi:10.1007/s10750-004-7475-7.

Phillips, R., and E. Meñez (1988), Seagrasses, *Smithsonian Contrib. Mar. Sci.*, *34*, Smithsonian Inst. Press, Washington, D. C.

Prager, E., and R. Halley (1999), The influence of seagrass on shell layers and florida bay mudbanks, *J. Coastal Res.*, *15*(4), 1151–1162.

Raubenheimer, B., R. T. Guza, and S. Elgar (1996), Wave transformation across the inner surf zone, *J. Geophys. Res.*, *101*(C11), 25,589–25,597.

Raubenheimer, B., R. T. Guza, and S. Elgar (2001), Field observations of wave-driven setdown and setup, *J. Geophys. Res.*, *106*(C3), 4629–4638.

Schanz, A., and H. Asmus (2003), Impact of hydrodynamics on development and morphology of intertidal seagrasses in the wadden sea, *Mar. Ecol. Prog. Ser.*, *261*, 123–134.

Sfriso, A., and P. Ghetti (1998), Seasonal variation in biomass, morphometric parameters and production of seagrasses in the lagoon of venice, *Aquat. Bot.*, *61*(3), 207–223.

Soulsby, R. (1997), *Dynamics of Marine Sands: A Manual for Practical Applications*, Thomas Telford, London.

Thornton, E. B., and R. T. Guza (1982), Energy saturation and phase speeds measured on a natural beach, *J. Geophys. Res.*, *87*(C12), 9499–9508.

Tonks, V. (2008), An investigation into the sediment processes on ryde sandflat using grain trend analysis, M.Sc., University of Southampton, Southampton, U. K.

Van Lent, F., P. Nienhuis, and J. Verschuure (1991), Production and biomass of the seagrasses *Zostera noltii Hornem.* and *Cymodocea nodosa*

(Ucria) Aschers. at the Banc d'Arguin (Mauritania, NW Africa): A preliminary approach, *Aquat. Bot.*, *41*(4), 353–368.

Verduin, J., J. Backhaus, and D. Walker (2002), Estimates of pollen dispersal and capture within *Amphibolis antarctica (Labill.) sonder* and *aschers. ex aschers.* meadows, *Bull. Mar. Sci.*, *71*(3), 1269–1277.

Ward, L., W. Kemp, and W. Boynton (1984), The influence of waves and seagrass communities on suspended particulates in an estuarine embayment, *Mar. Geol.*, *59*, 85–103.

Widdows, J., N. Pope, M. Brinsley, H. Asmus, and R. Asmus (2008), Effect of seagrass beds (*Zostera noltii* and *Z. marina*) on near-bed hydrodynamics and sediment resuspension, *Mar. Ecol. Prog. Ser.*, *358*, 125–136, doi:10.3354/meps07338.

C. L. Amos and M. Paul, National Oceanography Centre, University of Southampton, Waterfront Campus, European Way, Southampton SO14 3ZH, UK. (maike.paul@soton.ac.uk)